Вісник Харківського національного університету імені В. Н. Каразіна. Серія «Фізика». Вип. 43, 62–70 (2025)
Journal of V. N. Karazin Kharkiv National University. Series Physics. Iss. 43, 62–70 (2025)
ISSN 2222-5617 (Print)

Original article
In print article
https://doi.org/10.26565/2222-5617-2025-43-06
UDC 532.527 ; 532.54 ; 535.211 ; 535.214 ; 536.252
PACS numbers: 42.50.Wk ; 42.65.Jx ; 47.15.ki ; 47.20.-k ; 47.55.pb

MANIFESTATIONS OF VORTEX BEHAVIOR OF FLUIDS IN VARIOUS PHYSICAL EXPERIMENTS

A. O. Belova[1], V. I. Lymar[1], Ye. D. Makovetskyi[1], Yu. S. Malyi[2]

[1]*V. N. Karazin Kharkiv National University, 4 Svobody Sq., 61022 Kharkiv, Ukraine*
[2]*Lyceum No 34 of Kharkiv City Council, 2 Lokomotyvna Str., 61080 Kharkiv, Ukraine.*
E-mail: vilymar@karazin.ua

Received on October 10, 2025. Reviewed on November 19, 2025.
Accepted for publication on November 21, 2025. Published on November 26, 2025.

The paper presents a comprehensive examination of experimental manifestations of vortex behaviour in fluids, focusing on phenomena generated by physical mechanisms of fundamentally different nature. Through a systematic analysis of diverse hydrodynamic systems, this work demonstrates that nonlinear vortical dynamics represents an inherent and fundamental element of fluid motion across multiple spatial and temporal scales. The study employs a range of illustrative examples, beginning with Albert Einstein's classical "small experiment" and the formation and evolution of meanders in lowland river channels. These seemingly simple phenomena are shown to be governed by the same underlying principles that drive more complex hydrodynamic instabilities. Particular attention is devoted to the development of Rayleigh-Taylor-type vortical instabilities, which are characterized by the mutual "overturning" of heavy and light fluid components in a flowing medium. The paper explores these instabilities through experimental configurations, including thermal convection processes and the formation of "underwater crater" structures in granular materials settling through liquids. A central theoretical framework is established through the identification of common universal features of vortical excitations, all of which are fundamentally linked to the classical Helmholtz vortices in ideal fluid dynamics. The authors demonstrate that despite the diversity of mechanisms generating vortex behavior in real fluids, and the wide range of conditions under which such behavior manifests, there exist universal properties stemming from their connection to Helmholtz vortices. This unifying approach contributes significantly to the formation of a coherent theoretical framework capable of describing a remarkably broad spectrum of physical phenomena observed both in nature and in controlled laboratory experiments, from microscale optical self-defocusing patterns to astronomical structures like the Crab Nebula.

Keywords: *ideal fluid, vorticity field, hydrodynamic vortices, Rayleigh-Taylor instability, thermal convection, thermal self-defocusing.*

In cites: *A. O. Belova, V. I. Lymar, Ye. D. Makovetskyi, Yu. S. Malyi. Manifestations of vortex behavior of fluids in various physical experiments.* Journal of V. N. Karazìn Kharkiv National University. Series Physics. Iss. 43, 2025, X–XX. https://doi.org/10.26565/2222-5617-2025-43-06

INTRODUCTION

"The subject of the flow of fluids, and particularly of water, fascinates everybody. We can all remember, as children, playing in the bathtub or in mud puddles with the strange stuff. As we get older, we watch streams, waterfalls, and whirlpools, and we are fascinated by this substance which seems almost alive relative to solids…" – with these words Richard Feynman begins the hydrodynamics section of his famous "Lectures on Physics" [1]. Water, with its unique physical properties, is on the one hand the most vital life-supporting chemical compound for all living beings on our planet, and on the other – in its common liquid state – is perhaps one of the most enigmatic and, therefore, constantly studied objects in such branches of physics as hydromechanics and hydrodynamics.

In general, despite its long history of investigation, the liquid state of matter – as an intermediate between the solid and gaseous states – remains, to some extent, the least studied of the three. The fundamental properties of solids, liquids, and gases are directly related to their molecular structure and the nature of intermolecular forces. Their characteristic features for each state of matter are summarized in the table below [2].

State of matter	Intermolecular forces	Ratio of the amplitude of molecular thermal motion to the average inter-molecular distance	Arrangement of molecules
solid	strong	much less than 1	ordered with the presence of long-range order
liquid	intermediate	comparable with 1	partially ordered, short-range order only
gas	weak	much greater than 1	disordered, no long-range or short-range order

Evidently, due to the presence of intermolecular forces, liquids are "closer" to solids, while the influence of thermal motion gives liquid molecules a degree of freedom of movement that makes them similar to gases. Like solids, liquids retain their volume, but as with gases, they do not withstand shear stress, leading to their characteristic fluidity and the inability to preserve their shape. For this reason, when analyzing macroscopic motion under external forces, the difference in behavior between liquids and gases appears considerably less pronounced than that between liquids and solids. Consequently, both are treated within a unified mathematical framework of various hydro- and gas-dynamic models of a continuous fluid medium.

HELMHOLTZ VORTICES AS "NONLINEAR STRUCTURAL ELEMENTS" OF THE VELOCITY FIELD OF AN IDEAL FLUID MEDIUM

The above-mentioned complexity of hydrodynamics arises primarily from the intrinsic nonlinearity of the fluid motion equations which serve as the starting point for practically all dynamic problems. From the standpoint of the so-called Eulerian approach [3] , the motion of a fluid is described as a velocity field $\vec{\mathbf{v}}(t,\vec{\mathbf{r}})$ defined in a four-dimensional continuum where time t and spatial coordinates $\vec{\mathbf{r}}$ are independent variables. However, when we consider the motion of a specific fluid particle, its spatial coordinates $\vec{\mathbf{r}}(t)$ become functions of time. The particle's acceleration can then be written in the form of a total (substantial) derivative:

$$\frac{d\vec{\mathbf{v}}}{dt}(t,\vec{\mathbf{r}}) = \frac{\partial\vec{\mathbf{v}}}{\partial t} + (\vec{\mathbf{v}}\cdot\nabla)\vec{\mathbf{v}}. \qquad (1)$$

Here, ∇ is the Hamiltonian (nabla) operator in Cartesian coordinates. The first term represents the *local* contribution to acceleration, while the second term is called the *convective* component. It is precisely the presence of this convective term that becomes the "source of nonlinearity" in the hydrodynamic equation of fluid motion.

For our further consideration, it is useful to write the Euler–Helmholtz equation of motion for an *ideal incompressible* fluid as

$$\frac{\partial\vec{\boldsymbol{\omega}}}{\partial t} + \nabla\times(\vec{\boldsymbol{\omega}}\times\vec{\mathbf{v}}) = 0 \qquad (2a)$$

subject to

$$\vec{\boldsymbol{\omega}} = \nabla\times\vec{\mathbf{v}} \quad \text{and} \quad \nabla\cdot\vec{\mathbf{v}} = 0. \qquad (2b,c)$$

Equation (2b) defines the vector field $\vec{\boldsymbol{\omega}}(t,\vec{\mathbf{r}})$ of vorticity in an incompressible (Eq. (2c)) medium. The velocity field $\vec{\mathbf{v}}(t,\vec{\mathbf{r}})$ of the fluid "wraps" around the lines of the vorticity field $\vec{\boldsymbol{\omega}}(t,\vec{\mathbf{r}})$, whose density is proportional to the magnitude ω, while the tangents to these lines at each point $(t,\vec{\mathbf{r}})$ define the direction of $\vec{\boldsymbol{\omega}}$. The equation of motion (2a) acquires physical meaning as a nonlinear equation of self-consistent advection of vorticity lines of the field $\vec{\boldsymbol{\omega}}$ by the motion of an ideal incompressible fluid governed by its velocity field $\vec{\mathbf{v}}(t,\vec{\mathbf{r}})$ [4]. Based on these equations (2a–c), in 1858 Hermann Helmholtz formulated the following fundamental properties of nonlinear vortex excitations in such a model:

1) The circulation of velocity remains constant within a vortex.
2) In an initially irrotational fluid, vortices can only be generated in pairs with opposite circulations.
3) Vortex lines must be closed in an infinite medium or terminate at its boundaries.
4) A vortex line can be transported and deformed by the flow; its most stable configuration is a closed ring.
5) Two separate vortex lines can merge into a stable closed configuration.

Thus, the equations of hydrodynamics theoretically allow the existence of nonlinear vortex excitations of fluid motion – the Helmholtz vortices – possessing special properties under idealized conditions. The presence of vortices in real water streams or gusts of wind is confirmed by our everyday experience which, on the one hand, shows that the theory works (albeit with certain limitations), and on the other hand, that vortices are indeed typical structural elements of the velocity field $\vec{\mathbf{v}}(t, \vec{\mathbf{r}})$ of a fluid medium. In the cases discussed below, taking into account the vortex nature of such motion allows for a meaningful and qualitative explanation of physical phenomena that, at first glance, may appear unrelated.

EINSTEIN'S PROBLEM OF TEA LEAF MOTION IN A CUP AND RIVER MEANDERS

The question of the formation of meanders – bends in river channels – particularly noticeable in slowly flowing lowland rivers, began to attract the attention of scientists around the middle of the 19th century. However, it was Albert Einstein's consideration of this problem that gained particular popularity due to his clear and intuitive physical explanation of the phenomenon. One hundred years ago, on January, 7, 1926, at a meeting of the Prussian Academy of Sciences, Einstein presented his report "The Cause of the Formation of Meanders in River Courses and the So-Called Baer's Law" [5, 6]. Fig. 1 shows Einstein's original illustrations from his publication. Einstein began with a simple illustrative example:

"Let us start with a small experiment that anyone can repeat. Imagine a cup with a flat bottom filled with tea. A few tea leaves at the bottom remain there because they are slightly heavier than the water. If one uses a spoon to set the liquid into rotation, the leaves soon collect at the center of the cup's bottom. The explanation of this phenomenon is as follows: rotation of the liquid gives rise to centrifugal forces. These forces alone would not alter the flow pattern if the liquid were rotating as a rigid body. However, due to friction against the cup walls, the angular velocity of the liquid is smaller near the boundary

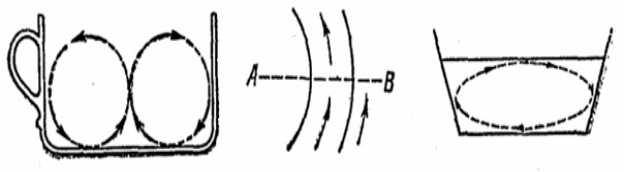

Fig. 1. Illustrations by A. Einstein from his article [5].

than near the center. In particular, the angular velocity – and therefore the centrifugal force – is smaller near the bottom than at higher levels. The result is a secondary vortex motion of the liquid, similar to that illustrated in Fig. 1 (left – auth.). This circulation develops until it becomes stationary under the influence of friction. The tea leaves are carried toward the center by this vortex flow, thus confirming its existence".

Fig. 2 [6] demonstrates the experiment described in the above quotation.

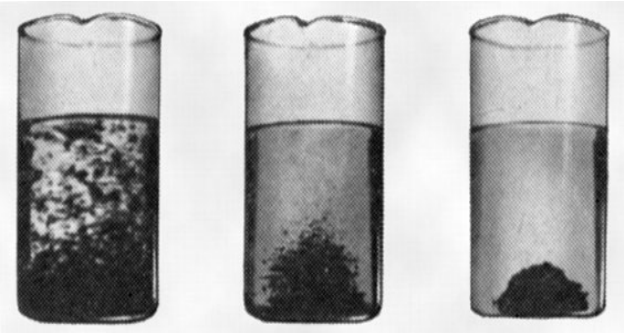

Fig. 2. Albert Einstein's "small experiment" [6].

Einstein then generalized this model, originally described for a cup of tea, to analyze the motion of water in a curved riverbed (see Fig. 1, center and right). In each cross-section of the river, a centrifugal force acts outward, from point **A** to point **B**. Because of friction, this force is reduced in the near-bank and bottom layers of the flow, leading to the formation of a secondary vortex motion, as shown in Fig. 1 (right). Moreover, even in regions where the river channel curvature is absent, the formation of a similar vortex pattern is possible due to the Earth's rotation. It produces the Coriolis force, whose horizontal component acts perpendicularly to the right of the flow direction, with a magnitude per unit mass given by $2\mathbf{v} \cdot \mathbf{\Omega} \cdot \sin\Phi$ where $\mathbf{v}$ is the flow velocity, $\mathbf{\Omega}$ is the angular velocity of Earth's rotation, and Φ is the geographical latitude. Due to friction with the riverbed, the near-bottom velocity $\vec{\mathbf{v}}$ decreases, causing a shear in velocity distribution that again induces rotational motion of the fluid, as shown in Fig. 1 (right). Taking into account the gradual erosion of the riverbed with associated mass transport, one can understand the emergence of asymmetry of riverbanks (Baer's law) and the enhancement of river meandering accompanied by the slow migration of meander bends downstream.

Thus, based on attentive everyday observation and the construction of a clear physical model of vortex formation in a fluid under the action of inertial and friction forces, A. Einstein qualitatively proposed a comprehensive and insightful description of the processes of river meandering and channel evolution. His explanation remains highly relevant today as a fundamental conceptual foundation for modern scientific and technical applications alike.

ON THE FORMATION OF VORTICES DURING THE DEVELOPMENT OF RAYLEIGH–TAYLOR INSTABILITY

Let us consider two layers of different fluids positioned one above the other in a gravitational field and separated by a horizontal interface [7]. For simplicity, we neglect viscosity and the presence of container walls. The only relevant quantities are the densities of the two fluids, ρ_1 and ρ_2, the surface tension coefficient σ, and the gravitational acceleration g (Fig. 3, left).

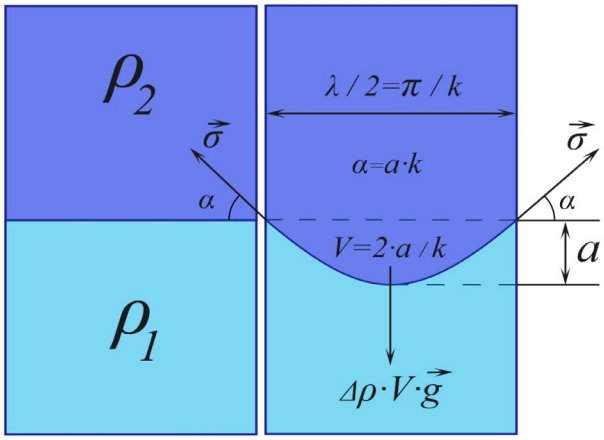

Fig. 3. Development of the Rayleigh–Taylor instability occurs under the condition that the Atwood number $A > 0$ ($\rho_2 > \rho_1$). The *right* panel schematically shows the forces of surface tension $\vec{\boldsymbol{\sigma}}$ and buoyancy $\Delta\rho V\vec{\mathbf{g}}$ ($\Delta\rho = \rho_2 - \rho_1$) acting on a half-wavelength sinusoidal perturbation of the fluid interface.

For this system, it is useful to introduce the so-called Atwood number

$$A = \frac{\rho_2 - \rho_1}{\rho_2 + \rho_1} \qquad (3)$$

and to analyze the balance between the buoyancy and surface tension forces when a half-wave $\lambda/2$ perturbation of the interface arises in the form $a \sin kx$ where $k = 2\pi/\lambda$ (see Fig. 3, right). If $\rho_2 > \rho_1$, then the buoyancy force dominates the surface tension at spatial scales λ satisfying

$$\lambda \geq \pi\sqrt{\sigma/(g \cdot \Delta\rho)}. \qquad (4)$$

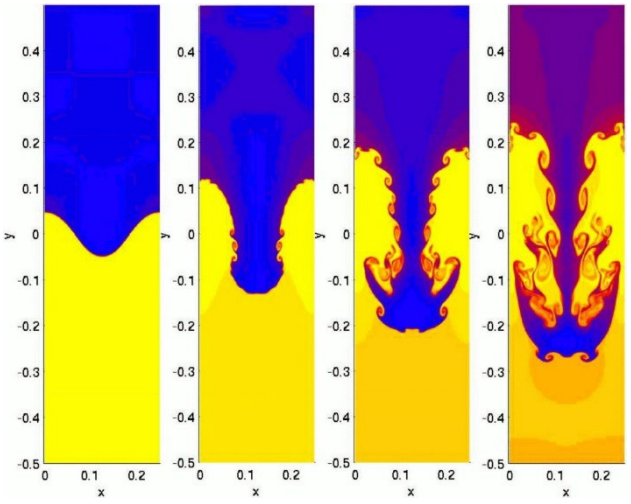

Fig. 4. Computer simulation of the evolutionary development of the Rayleigh-Taylor instability [8]. The penetration of the denser fluid (*upper blue*) into the lighter fluid (*lower yellow*) occurs through the formation of a large-scale mushroom-shaped protrusion. The small-scale vorticities are consequences of the development of the so-called Kelvin-Helmholtz instability.

Hence, the essence of the Rayleigh-Taylor instability lies in the following: when $A > 0$, the interface between the two fluids becomes unstable to perturbations with spatial scales λ that satisfy inequality (4).

Fig. 4 illustrates a numerical simulation of the penetration of the denser fluid (*blue, top*) into the lighter one (*yellow, bottom*) under Rayleigh–Taylor instability conditions [8]. An initially smooth, nearly sinusoidal interface (as in Fig. 3, right) gradually transforms into a large-scale mushroom-shaped protrusion due to mutually reinforcing flows on both sides of the deformation which exhibit noticeable vorticity on large scales consistent with (4). The evolution pattern in Fig. 4 is further complicated by the emergence of small-scale Kelvin–Helmholtz vortices. The Kelvin–Helmholtz instability is responsible for the generation of vortical waves at the interface between two moving media. We naturally observe the outcome of this instability on the water surfaces of seas and oceans where wind induces wave formation.

Phenomena of convection – the appearance of fluid flows driven by non-uniform heating – can also be regarded as a manifestation of the Rayleigh–Taylor instability, but under conditions of nearly zero Atwood number $A \to 0$ and effectively infinite miscibility [9]. The development of convective instability occurs when the pressure gradient ∇p in the liquid, related to gravitational acceleration g, combines with the density gradient $\nabla\rho$ according to the inequality:

$$\nabla p \nabla \rho < 0. \qquad (5)$$

In the case of a two-dimensional convective structure in an ideal fluid, the behavior of the vorticity field $\vec{\boldsymbol{\omega}}(t, \vec{\mathbf{r}})$ of flow lines is described by the following equation [9, 10]:

$$\frac{d\vec{\boldsymbol{\omega}}}{dt}(t, \vec{\mathbf{r}}) = \frac{1}{\rho^2}\nabla\rho \times \nabla p. \qquad (6)$$

The definition of vorticity $\vec{\boldsymbol{\omega}}(t, \vec{\mathbf{r}})$ (see Eq. (2b)) still applies here, and the vector $\vec{\boldsymbol{\omega}}$ is double the value of the angular velocity of the fluid particle located at point $(t, \vec{\mathbf{r}})$. Equation (6) shows that at any point in the fluid where the gradients of pressure and density are not parallel, a hydrodynamic torque arises, known as a baroclinic vortex [10]. This torque causes local rotational acceleration of fluid particles, leading to the formation of vortices similar to those illustrated in Einstein's "small experiment" (Fig. 1, left).

A clear manifestation of such vortices can be observed in the course of a nonlinear optical experiment [11]. A laser beam with a symmetric transverse Gaussian intensity profile is focused at the entrance to a thin (~1 mm) layer of a light-absorbing liquid. Heating and thermal expansion of the medium produce, on the one hand, a thermal lens – a region with a decreased refractive index – leading to nonlinear optical self-defocusing of the beam. On the other hand, the same heating and expansion processes promote the development of the Rayleigh–Taylor-type instability of the quiescent liquid. This instability is essentially baroclinic in nature, and its mechanism is schematically illustrated in Fig. 5 (in the plane perpendicular to the laser beam). In the upper portion of the irradiated region where condition (5) is satisfied, two baroclinic convective vortices are formed with opposite directions of vorticity (in accordance with the list of Helmholtz vortex properties, item two). The velocity fields of these vortices coincide slightly above the laser beam's center; therefore, according to Bernoulli's principle, this vortex pair constitutes a stable convective structure after a transient, threshold-free convection onset (as far as in the inequality (4) the lowest limit of λ is tended to zero at $\sigma \to 0$). In the steady state, the fields of flow velocity and vorticity evidently adjust to minimize the hydrodynamic torque and stabilize the flow pattern in the system. The convective flows influence on the diffraction of the laser beam that induces them and the self-consistent result of this process is manifested in the observed thermal self-defocusing pattern shown in Fig. 6. Before the excitation of convective vortices, at the initial moment of illumination, the self-defocusing pattern exhibits an approximately circular symmetry (Fig. 6, right), consistent with the Gaussian beam intensity distribution. After a transient oscillatory process lasting typically several seconds, the pattern becomes deformed and evolves into a stationary structure (Fig. 6, left). According to the discussion above, this stationary self-defocusing pattern corresponds to the established convective flow field in the form of a pair of baroclinic vortices.

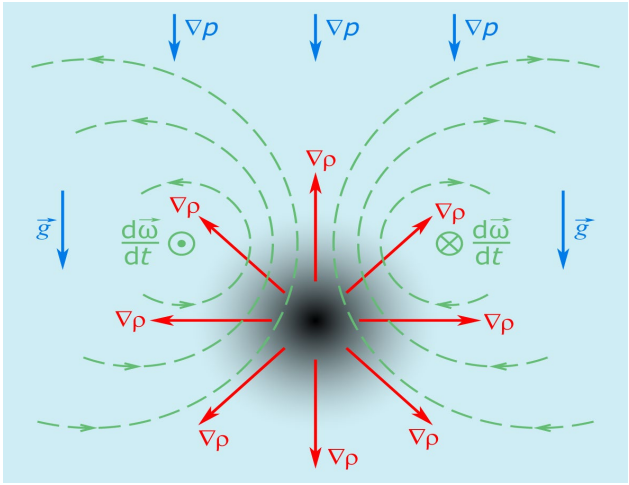

Fig. 5. Origin of a pair of baroclinic vortices (green dashed lines) in a "free" convective flow induced by a focused Gaussian laser beam: ∇p – pressure gradient vector associated with gravity $\vec{\mathbf{g}}$; $\nabla\rho$ – density gradient vector arising from local heating of the absorbing liquid; the shaded region represents the laser-heated zone with reduced density and refractive index. The structure of vortices is similar to the one illustrated in A. Einstein's Fig. 1 (left).

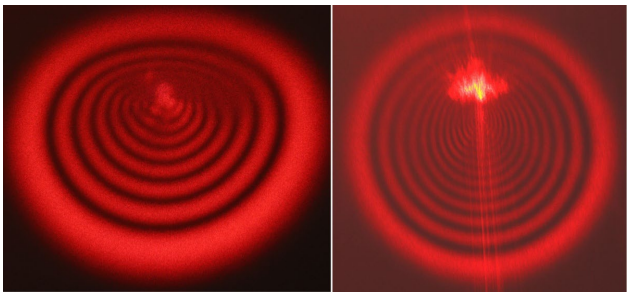

Fig. 6. Comparison of light self-defocusing patterns ("at the output," after beam propagation through the liquid layer) in the presence of a convective flow (*left*) and in the "pre-convective" state before convection onset (*right*).

ON ANOTHER "SMALL EXPERIMENT" AND THE MANIFESTATION OF RAYLEIGH-TAYLOR INSTABILITY

For the 39th International Young Physicist' Tournament (IYPT) to be held in July 2026 in Zurich (www.iypt.org), one of the proposed problems is Problem 10 "Underwater Crater", formulated as follows: "If you release sand or similar granular material in a container filled with water, the material will sink to the bottom and may form a crater-like structure. Explain and investigate

the phenomenon". A video demonstration of the experiment is also available on the website [12]. Since the Young Physicists' Tournament has already taken place in Kharkiv, we find it appropriate to analyze certain aspects of the physical mechanisms behind this "small experiment" in the context of our general discussion.

In the photograph shown in Fig. 7, one can observe a quasi-ring-shaped distribution of fine salt grains on the bottom of the water container, formed when the total amount of salt is relatively small (a few grams). We suggest that this ring-like structure arises from the formation of a toroidal vortex in the water during the descent of the granular material, in accordance with the fourth Helmholtz vortex property (see the second section). In a quasi-continuous approximation, the collective motion of many salt grains falling through the water can be regarded as the flow of a fluid with an effective mean density greater than that of water. Under these conditions, the Rayleigh-Taylor instability model, analyzed in the preceding section, becomes applicable. The approximate qualitative distributions of the pressure gradient ∇p and density gradient $\nabla \rho$ fields are shown schematically in Fig. 8 for the case when a small portion of salt is settling onto the bottom of the container (note that, unlike Fig. 5, the darker region here corresponds to increased density ρ). According to Eq. (5), the condition for Rayleigh-Taylor instability is also fulfilled in this configuration. In line with Eq. (6), in the vertical cross-section, a pair of vortices is generated – similar to those shown in both Fig. 1 and Fig. 5 – but with opposite vorticity $\vec{\boldsymbol{\omega}}$ sign and opposite flows $\vec{\mathbf{v}}(t, \vec{\mathbf{r}})$ depicted by green dashed arrows. Thus, in this case, we may speak of Einstein's "small anti-effect": salt particles are captured by the vortex motion of the water and carried from the center outward to the periphery, opposite to the behavior of the tea leaves in Einstein's "small experiment" in Fig. 2. But the degree of nonlinearity of "anti-effect" is, of course, higher, since the motion of salt grains must be dynamically coupled to the fluid velocity field – i.e., both movements have to be self-consistent.

When the amount of salt (or the granular material flux) is increased, the quasi-ring pattern becomes blurred, and a significant portion of the salt remains near the center, not entrained by the toroidal vortex (Fig. 9, left). This behavior can be explained by the increasing influence of viscous friction as the material flux grows. With greater homogeneity near the axis of the descending flow – that is, with a smaller density gradient $\nabla \rho$ in the center of the flux – the resulting vorticity distribution becomes more non-uniform at the periphery. Then, the right-hand side of Eq. (6) must include an additional diffusion term of the form $(\eta/\rho)\Delta\vec{\boldsymbol{\omega}}$ where η is the fluid viscosity and Δ is the Laplacian operator [1]. As a consequence, the vortex structure tends to form predominantly on the periphery of the granular jet rather than in its center, and due to vorticity diffusion, it simultaneously loses sharpness – just as a smoke ring fades and disperses as it expands. This qualitative reasoning explains the differences in the observed structures in Fig. 9 (left) and in Fig. 7.

Interestingly, as the downward flux increases, the pattern of salt particle distribution on the container bottom becomes in some sense analogous to the filamentary

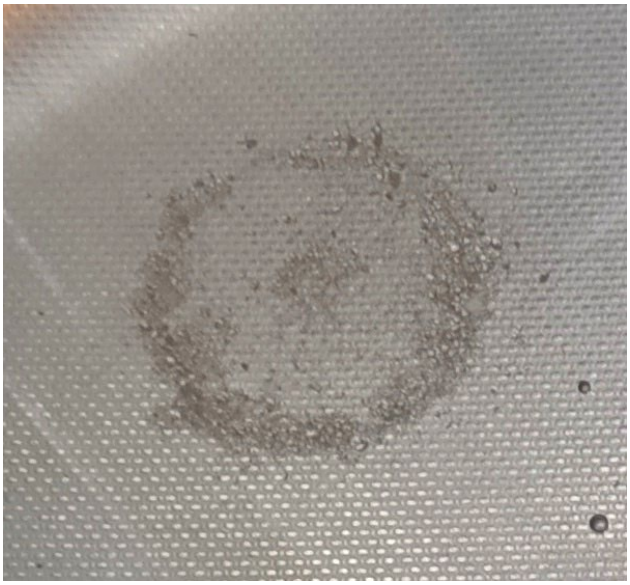

Fig. 7. Appearance of an "underwater crater" formed by fine-grained salt. The averaged diameter of the structure is approximately 4 cm, with a water depth of about 5 cm.

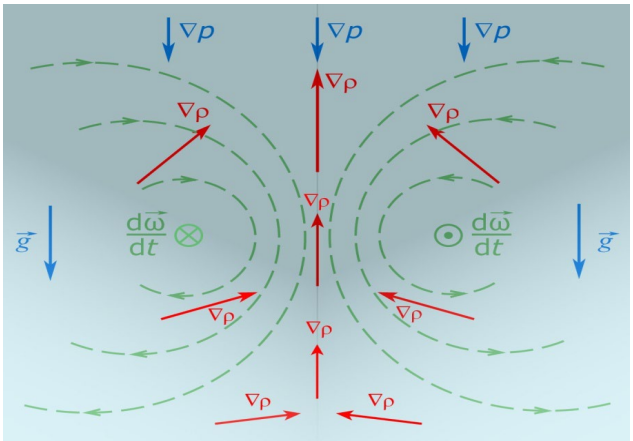

Fig. 8. Schematic illustration of Rayleigh-Taylor instability development in a vertical axis cross-section of the "underwater crater" experiment. A pair of counter-rotating vortices $\vec{\boldsymbol{\omega}}$ is formed – opposite in orientation to those in Fig. 1 and Fig. 5. The darker upper region corresponds to higher density ρ due to the larger concentration of salt grains.

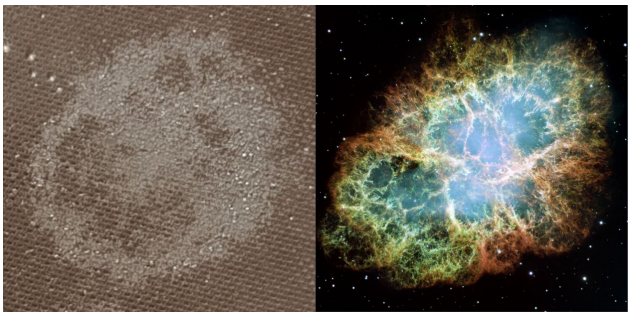

Fig. 9. Structure of the “underwater crater” at larger granular fluxes (*left*). Filamentary structure of the Crab Nebula (NGC 1952), generally interpreted as a result of Rayleigh-Taylor instability during the supernova explosion (*right*).

structure observed in the Crab Nebula (NGC 1952) [13] (see Fig. 9 (right)). Despite the enormous differences in physical processes, scales, and conditions responsible for such vastly distinct structures, the Rayleigh-Taylor instability emerges as a common and fundamental mechanism governing both phenomena. This similarity may be viewed as evidence of the universality and validity of physical laws throughout the natural world, across all spatial and temporal scales. Following the inspiring example of Albert Einstein, we explore and understand nature through our own “small experiments,” simultaneously gaining insight into the Universe.

CONCLUDING REMARKS

In the pre-Galilean era, the study of mechanical motion appeared almost intractable due to the wide diversity of its manifestations and the multitude of causes that generated it. The complexity seemed overwhelming, with different types of motion – falling bodies, projectiles, planetary orbits, pendulum oscillations – appearing to obey entirely different laws. It took the genius of Galileo Galilei to conceive an idealized world in which frictional forces could be neglected, allowing him to formulate the law of inertia and the principle of relativity for mechanical motion. This revolutionary conceptual breakthrough provided mechanics with its fundamental "point of support," from which both its steady methodical progress and the subsequent advancement of all physics began. The power of Galileo's approach lay not in denying the existence of friction, but in recognizing that the essential features of motion could be understood by first studying the ideal case and then treating real-world complications as perturbations.

To a considerable extent, an analogous situation exists in fluid dynamics. Real fluids are universally characterized by the presence of viscous forces, which introduce dissipation, energy loss, and complex boundary layer effects into the dynamics. The absence of such viscous forces corresponds to the idealized theoretical model of a perfect (ideal) fluid – a construct that, while physically unrealizable in most circumstances, provides the conceptual foundation for understanding fluid behavior. Of course, there are remarkable special cases – such as superfluid helium at temperatures below the lambda point or Bose-Einstein condensates of ultracold atomic gases – whose exotic quantum nature allows them to exhibit genuine superfluid behavior. These extraordinary systems represent fascinating exceptions that ultimately confirm the rule regarding the prevalence of viscosity in conventional fluids.

Nevertheless, within the mathematical framework of an ideal incompressible fluid, the general solution of the hydrodynamic equations can be elegantly expressed in terms of Helmholtz vortices, which constitute the fundamental *modus operandi* of an ideal fluid medium. These vortical structures possess well-defined topological properties, conservation laws, and evolutionary dynamics that make them the natural "building blocks" for describing fluid motion.

The general approach of the present work was to demonstrate that, despite the remarkable diversity of physical mechanisms giving rise to vortex behavior in real fluids, and despite the wide range of conditions under which such behavior manifests itself under various departures from ideality – including viscous dissipation, thermal effects, and interfacial phenomena – there exist profound universal properties of vortical excitations. These properties stem directly from their "genetic linkage" to the Helmholtz vortices of ideal fluid theory. Establishing this fundamental connection helps to form a unified and coherent physical picture of many natural phenomena observed across vastly different scales and contexts, from laboratory experiments to geophysical and astrophysical systems, in which vortical motion in gases and liquids plays an important, and perhaps even decisive, role in determining the overall dynamics and evolution of the system.

CONFLICT OF INTEREST

The authors declare that they have no conflict of interests.

КОНФЛІКТ ІНТЕРЕСІВ

Автори повідомляють про відсутність конфлікту інтересів.

СПИСОК ВИКОРИСТАНИХ ДЖЕРЕЛ

1. R. P. Feynman, R. B. Leighton, M. Sands. The Feynman Lectures on Physics, Addisson-Wesley Pub. Co., Reading-London, (1963-1965).
2. G. K. Batchelor. An Introduction to Fluid Dynamics, Cambridge University Press, Cambridge (1967), 615 p.
3. L. D. Landau, E. M. Lifshitz. Fluid Mechanics, Pergamon Press, Oxford – Toronto (1987), 539 p.

4. А. В. Тур, В. В. Яновський. Гідродинамічні вихрові структури, НТК «Інститут монокристалів» НАН України, Харків (2012), 294 с.
5. A. Einstein, Naturwissenschaften, 14, p. 223 (1926).
6. А. А. Варламов, Л. Г. Асламазов. Несамовита фізика: піца, скрипка, вино і надпровідність, наш формат, Київ (2020), 400 с.
7. F. Charru. Hydrodynamic Instabilities, Cambridge University Press, Cambridge (2011), 391 p.
8. Shengtai Li, Hui Li. Parallel AMR Code for MHD/HD Equations, Techn. Rep. LA-UR-03-8926, Los Alamos National Lab., Los Alamos (2003), 2 p.
9. M. S. Roberts, J. W. Jacobs. Journal of Fluid Mech., 787, 50 (2016). https://doi.org/10.1017/jfm.2015.599
10. P. K. Kundu, I. M. Cohen, D. R. Dowling. Fluid Mechanics, Elsevier Inc., Amsterdam-Tokyo (2016), 922 p.
11. A. O. Belova, V. I. Lymar, Y. D. Makovetskyi, M. L. Pogrebnyak and A. S. Rudenko. 2019 IEEE 8th International Conference on Advanced Optoelectronics and Lasers (CAOL), Bulgaria, 2019, p. 498. https://doi.org/10.1109/CAOL46282.2019.9019417.
12. https://youtube.com/shorts/qAPqEtucVPo
13. J. J. Hester. Annual Review of Astronomy and Astrophysics, 46, 127 (2008). https://doi.org/10.1146/annurev.astro.45.051806.110608

REFERENCES

2. R. P. Feynman, R. B. Leighton, M. Sands. The Feynman Lectures on Physics, Addisson-Wesley Pub. Co., Reading-London, (1963-1965).
2. G. K. Batchelor. An Introduction to Fluid Dynamics, Cambridge University Press, Cambridge (1967), 615 p.
3. L. D. Landau, E. M. Lifshitz. Fluid Mechanics, Pergamon Press, Oxford – Toronto (1987), 539 p.
4. A. V. Tur, V. V. Yanovsky. Hydrodynamical Vortical Structures, SSI „Institute for Single Crystals“ NASU, Kharkiv (2012), 294 p. (In Ukrainian).
5. A. Einstein, Natural Sciences, 14, p. 223 (1926). (in German).
6. A. A. Varlamov, L. G. Aslamazov. Crazy Physics: Pizza, Violin, Wine and Superconductivity, Nash Format, Kyiv (2020), 400 p. (In Ukrainian).
7. F. Charru. Hydrodynamic Instabilities, Cambridge University Press, Cambridge (2011), 391 p.
8. Shengtai Li, Hui Li. Parallel AMR Code for MHD/HD Equations, Techn. Rep. LA-UR-03-8926, Los Alamos National Lab., Los Alamos (2003), 2 p.
9. M. S. Roberts, J. W. Jacobs. Journal of Fluid Mech., 787, 50 (2016). https://doi.org/10.1017/jfm.2015.599
10. P. K. Kundu, I. M. Cohen, D. R. Dowling. Fluid Mechanics, Elsevier Inc., Amsterdam-Tokyo (2016), 922 p.
11. A. O. Belova, V. I. Lymar, Y. D. Makovetskyi, M. L. Pogrebnyak and A. S. Rudenko. 2019 IEEE 8th International Conference on Advanced Optoelectronics and Lasers (CAOL), Bulgaria, 2019, p. 498. https://doi.org/10.1109/CAOL46282.2019.9019417.
12. https://youtube.com/shorts/qAPqEtucVPo
13. J. J. Hester. Annual Review of Astronomy and Astrophysics, 46, 127 (2008). https://doi.org/10.1146/annurev.astro.45.051806.110608

ПРОЯВ ВИХРОВОЇ ПОВЕДІНКИ РІДИН У РІЗНИХ ФІЗИЧНИХ ЕКСПЕРМЕНТАХ

А. О. Бєлова[1], В. І. Лимар[1], Є. Д. Маковецький[1], Ю. С. Малий[2]

[1]Харківський національний університет ім. В. Н. Каразіна, пл.. Свободи, 4, 61022 Харків, Україна
[2]Комунальний заклад «Харківський ліцей №34 Харківської міської ради» м. Харкова, вул.. Локомотивна, 2, 61080 Харків, Україна
E-mail: vilymar@karazin.ua

Надійшла до редакції 10 жовтня 2025 р. Переглянуто 19 листопада 2025 р.
Прийнято до друку 21 листопада 2025 р. Опубліковано 26 листопада 2025 р.

У статті надається різнобічний розгляд проявів вихрової поведінки рідин, які породжуються різними за своєю природою фізичними причинами. Проведений у роботі послідовний аналіз гідродинамічних систем демонструє, що нелінійна вихрова динаміка є невід'ємною і фундаментальною складовою руху рідини на різних просторових та часових масштабах. Розгляд включає низку ілюстративних прикладів, починаючи від класичного «маленького експерименту» Альберта Ейнштейна та меандрування русел рівнинних річок. Вказані, на перший погляд прості, явища регулюються спільними фізичними принципами, які є справедливими і для інших більш складних видів гідродинамічних нестійкостей. Особлива увага приділяється розвитку вихрової нестійкості Релея-Тейлора, яка характеризується взаємним «перевертанням» важкої і легкої компонент плинного середовища. Досліджується прояв цієї нестійкості в експериментах з лазерно-індукованою тепловою конвекцією та із формуванням структури типу «підводного кратера» при осіданні сипучого гранулярного матеріалу на дно контейнера з рідиною. Встановлення спільних універсальних особливостей вихрових збуджень, пов'язаних із ідеальними вихорами Гельмгольца, сприяє формуванню єдиної точки зору для розгляду вказаних вище гідродинамічних ефектів. Такий теоретичний підхід є придатним до застосування при аналітичному розгляді широкого спектру фізичних явищ, які спостерігаються як у звичайних природних умовах, так і при постановці лабораторних експериментів, від мікроскопічного теплового оптичного самодефокусування до формування волокнистої структури типу розподілу залишків вибуху наднової у астрономічній Крабоподібній туманності.

Ключові слова: *ідеальна рідина, поле завихреності, гідродинамічні вихори, нестійкість Релея-Тейлора, теплова конвекція, теплове самодефокусування.*